ORIGINAL PAPER

Colorimetric method for enzymatic screening assay of ATP using Fe(III)-xylenol orange complex formation

Akihiko Ishida · Yasuko Yamada · Tamio Kamidate

Abstract In hygiene management, recently there has been a significant need for screening methods for microbial contamination by visual observation or with commonly used colorimetric apparatus. The amount of adenosine triphosphate (ATP) can serve as the index of a microorganism. This paper describes the development of a colorimetric method for the assay of ATP, using enzymatic cycling and Fe(III)-xylenol orange (XO) complex formation. The color characteristics of the Fe(III)-XO complexes, which show a distinct color change from yellow to purple, assist the visual observation in screening work. In this method, a trace amount of ATP was converted to pyruvate, which was further amplified exponentially with coupled enzymatic reactions. Eventually, pyruvate was converted to the Fe(III)-XO complexes through pyruvate oxidase reaction and Fe(II) oxidation. As the assay result, yellow or purple color was observed: A yellow color indicates that the ATP concentration is lower than the criterion of the test, and a purple color indicates that the ATP concentration is higher than the criterion. The method was applied to the assay of ATP extracted from *Escherichia coli* cells added to cow milk.

Keywords Microbial contamination · ATP assay · Colorimetry · Enzymatic cycling · Xylenol orange · *Escherichia coli*

A. Ishida (✉) · Y. Yamada · T. Kamidate
Division of Biotechnology and Macromolecular Chemistry,
Graduate School of Engineering, Hokkaido University,
Nishi 8, Kita 13,
Sapporo 060-8628, Japan
e-mail: ishida-a@eng.hokudai.ac.jp

Abbreviations

ACES	N-(2-acetamido)-2-aminoethanesulfonic acid
ADP	adenosine 5′-diphosphate
AK	adenylate kinase
AMP	adenosine 5′-monophosphate
ATP	adenosine 5′-triphosphate
Hepes	N-(2-hydroxyethyl)piperazine-N'-ethanesulfonic acid
HK	hexokinase
LOD	limit of detection
PEP	phosphoenol pyruvate
PK	pyruvate kinase
XO	xylenol orange

Introduction

Recently, the need for the assay of microorganisms has been growing in the field of hygiene management, such as food production and product packaging. The amount of adenosine 5′-triphosphate (ATP) as well as the number of microorganisms in food products and manufacturing environments have served as the hygiene index. For the assay of ATP, the firefly bioluminescence method is typically used [1–6]. This method provides rapid analytical results with high sensitivity and selectivity with dedicated apparatus. On the other hand, there is strong demand for screening methods for assays of microorganisms or ATP with a visual observation method or with commonly employed colorimetric apparatus. Biological test kits with visual observation are commercially available. These test methods allow the identification of a specific strain of bacteria. However, the methods require 1–2 days because they involve cultivation of bacteria. For the colorimetric assay of ATP there are only a few enzymatic methods, in which ATP is

directly converted to a colored compound [7, 8]. In addition, the approaches for molecular recognition of ATP using synthesized chromogenic sensors have also been studied [9–11]. The sensors had high selectivity for the ATP anion and the binding to ATP was accompanied by a change of the visible spectra. The features of these sensors offer simple methods for ATP detection. However, the limits of detection (LODs) with the enzymatic assays and the molecular sensors were in the range 10^{-6}–10^{-8} M, which were higher than the target ATP concentrations (less than nanomolar levels) in the assay for microbial contamination. These LODs were related to the absorption coefficients (around 20,000 M^{-1} cm^{-1}) of the colored compounds or the sensors. Therefore, these colorimetric approaches had the limitation of sensitivity.

To overcome the limitation in the colorimetric methods, preconcentration or amplification of ATP is essential. For amplification of ATP, enzymatic cycling using the coupled hexokinase (HK)/pyruvate kinase (PK) system and the coupled adenylate kinase (AK)/PK system was studied and applied to the bioluminescence assay [12–15]. In the HK/PK system, ATP is degraded to adenosine 5′-diphosphate (ADP) by HK and ATP is also regenerated from ADP by PK [16]. This cycling results in accumulation of glucose 6-phosphate and pyruvate. In the AK/PK system, AK converts adenosine 5′-monophosphate (AMP) and ATP molecules to two molecules of ADP and then PK converts ADP to ATP. Thus, this cycling was considered as an amplifier of ATP that produces two molecules of ATP from one molecule of ATP [17]. This cycling is also accompanied by exponential accumulation of pyruvate. The theoretical studies demonstrated that the AK/PK system was more useful than the HK/PK system for the assay of ATP [17, 18]; thus, the AK/PK cycling was employed in this study.

When this enzymatic cycling is used, the initial ATP concentration can be determined indirectly by measuring pyruvate concentration using an indicator reaction. For determination of pyruvate, a variety of reactions are available, but most of the reactions are not fit for the purpose for visual screening. Typically, the indicator reactions for pyruvate involve the generation of H_2O_2 with pyruvate oxidase, followed by a peroxidase condensation between 4-aminoantipyrine and a hydrogen-donor chromogenic reagent [19–21]. The condensation produces a colored compound in proportion to H_2O_2 concentration, which results in a monochromatic change, i.e., a change only in color density (not kinds of color). The monochromatic color change is useful for quantitative assay with photometric apparatus; however, it would be difficult to compare colors with a standard color series in the visual test. Particularly for screening purposes, a color change with different kinds of colors, as seen in pH test strips,

would be preferable. The assay would be performed more easily, based on the difference in color. In this study, for the production of a colored compound from H_2O_2 produced in pyruvate oxidase reaction, Fe(III)-xylenol orange (XO; Fig. 1a) complex formation was used. In this method the complex formation followed the oxidation of Fe(II) to Fe(III) by H_2O_2 in the presence of XO, which provided the distinct color change from yellow to purple, depending on the Fe(III) concentration [22]. Furthermore, the color change can be designed so that a purple color is observed at an ATP concentration equal to and above the criterion of the screening and a yellow color is observed below the criterion. Thereby, samples with concentrations above the criterion can be clearly recognized by visual observation. Although the Fe(III)-XO complex formation has been used for the detection of H_2O_2 and peroxides (FOX method) [23–28], the characteristic color change of the complexes has not been exploited.
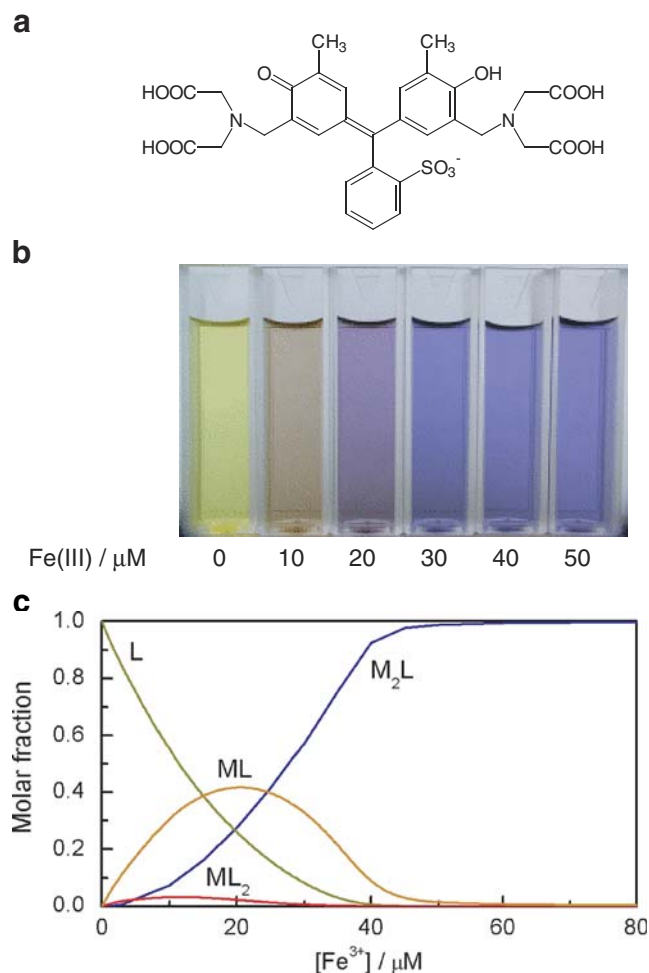
Fig. 1 **a** Xylenol orange (XO). **b** Color development and **c** calculated molar fraction of the Fe(III)–XO system as a function of Fe(III) concentration at a XO concentration of 20 μM

This paper describes the development of a colorimetric method for a screening assay of ATP using AK/PK cycling and Fe(III)-XO complex formation. We demonstrate the utility of the present assay by performing the assay of ATP extracted from *Escherichia coli* cells.

Materials and methods

Reagents

Ammonium iron(II) sulfate hexahydrate, potassium phosphoenol pyruvate (PEP), and peroxidase from horseradish (EC 1.11.1.7) were purchased from Wako Pure Chemical Industries (Japan). ATP disodium salt, AMP, AK from rabbit muscle ammonium sulfate suspension (EC 2.7.4.3), PK from rabbit muscle (type II, EC 2.7.1.40), and apyrase from potato (grade I, EC 3.6.1.5) were obtained from Sigma-Aldrich. *N*-(2-Acetamido)-2-aminoethanesulfonic acid (ACES) and 3,3′-bis[*N,N*-bis(carboxymethyl)amino-methyl]-*o*-cresolsulfonphthalein disodium salt (XO) were obtained from Dojindo Laboratories (Japan). Pyruvate oxidase (EC 1.2.3.3) was obtained from Toyobo (Japan).

An AMP stock solution was incubated with 2 U/mL apyrase at 37 °C for 60 min to reduce the ATP and ADP contained in the AMP stock solution as contaminants. This solution was then heated at 95 °C for 10 min to inactivate apyrase. The solution was cooled to room temperature and then stored at 4 °C. All other chemicals were used without further purification. Stock solutions of ammonium iron sulfate were prepared in 0.1 M HCl and were kept at 4 °C. XO stock solutions were prepared by dissolving the dry reagent in water. The Fe/XO reagent solution containing 4 mM Fe^{2+}, 40 μM XO, and 35 mM HCl was prepared daily using stock solutions. All solutions were prepared with ultrapure deionized water from a Millipore Milli-Q water purification system.

Preparation of *E. coli* samples

For the preparation of *E. coli* samples, *E. coli* strain KT1008 was used. The culture was grown in Luria–Bertani broth overnight at 37 °C. The culture was diluted 1:100 with fresh Luria–Bertani broth and was grown to mid log phase (optical density at 600 nm of approximately 0.4). The optical density at 600 nm was measured with a Hitachi U-1000 spectrophotometer with a 1 cm × 1 cm cell. The bacterial cells were collected by centrifugation at 10,000 *g*, for 5 min. The pellet was suspended in 25 mM *N*-(2-hydroxyethyl)piperazine-*N*′-ethanesulfonic acid (Hepes) buffer. The cell density was determined from the optical density of the cell suspensions, based on the optical density at 600 nm of 1.0, corresponding to 2.0×10^8 cells/mL.

Working cell suspensions were prepared by serial dilution with 25 mM Hepes buffer solution. All *E. coli* suspensions were stored on a crushed-ice bath until the extraction of ATP from *E. coli* cells.

The cell suspensions were added to commercially available cow milk to give cell concentrations of 5×10^5 and 1×10^6 cells/mL in the amplification reaction (total volume, 1.0 mL). These samples were mixed with 25% trichloroacetic acid (500 μL) and incubated for 5 min. Then, the mixtures were centrifuged at 8,000 *g* for 5 min. The supernatant (200 μL) of each sample was neutralized using NaOH and was diluted in 1.0 mM Hepes buffer (final volume, 2.0 mL).
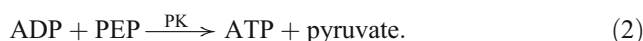
Colorimetric assay of ATP

To an ACES buffer (pH 7.8) containing AMP, PEP, and AK, the ATP solution was added. Then, a PK solution was immediately added to initiate the amplification reaction. The reaction mixture was composed of 0–10 nM ATP, 50 μM AMP, 500 μM PEP, 1.86 U/mL AK, 1.86 U/mL PK, and 0.15 M ACES at pH 7.8. After the incubation in a thermostated bath at 25°C for 45 min, a 1-mL portion of the reaction mixture was transferred to a glass cuvette. Then, 0.36 M HCl solution (325 μL) and 8.88 U/mL pyruvate oxidase (675 μL) were added to the cuvette and the mixture was incubated at pH 5.5 for 5 min. Next, the Fe/XO reagent (2 mL) was immediately added to the cuvette. After 5 min, the absorbance of the mixture was measured at 585 nm using a U-2000 spectrophotometer (Hitachi, Japan) equipped with a temperature-controlled chamber at 25 °C.
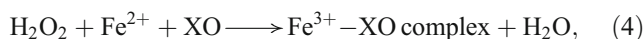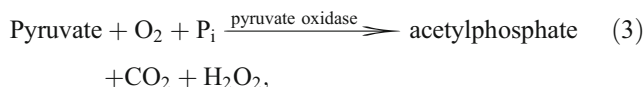
Results and discussion

Design and development of standard procedure

The present assay was based on the following reactions.
Amplification reaction:

$$ATP + AMP \xrightarrow{\text{AK}} 2ADP, \tag{1}$$

$$ADP + PEP \xrightarrow{\text{PK}} ATP + pyruvate. \tag{2}$$

Indicator reaction:

$$Pyruvate + O_2 + P_i \xrightarrow{\text{pyruvate oxidase}} acetylphosphate \quad (3)$$
$$+ CO_2 + H_2O_2,$$

$$H_2O_2 + Fe^{2+} + XO \longrightarrow Fe^{3+} - XO\,complex + H_2O, \quad (4)$$

where P_i is inorganic phosphate. In this assay, the presence of ATP initiates the AK/PK cycling and accumulates

pyruvate (Eqs. 1 and 2). The concentration of pyruvate accumulated increases with increasing initial ATP concentration. Next, pyruvate accumulated in the cycling is converted to H_2O_2 by pyruvate oxidase (Eq. 3). Finally, H_2O_2 oxidizes Fe(II), followed by the formation of XO–Fe (III) complexes (Eq. 4) [19]. Fe(III) ion forms complexes with XO under acidic conditions (pH 2.0), although Fe(II) ion does not form a complex. In addition, the other metal ions (100 μM Al^{3+}; 10 mM Mg^{2+}, Mn^{2+}, Co^{2+}, Ni^{2+}, Cu^{2+}, and Zn^{2+}) also showed no color change, which indicates very small stability constants with XO under those conditions. Figure 1b shows the color characteristics of the Fe(III)–XO complexes formed by adding various concentrations of Fe(III) ion to XO. The Fe(III)–XO complexes show two distinctly different colors, i.e., yellow and purple, although the color included a narrow intermediate color (reddish color). By using these color characteristics, one can design the colorimetric assay so that the yellow or reddish color can be observed at ATP concentrations below a screening criterion and the purple color at ATP concentrations above the criterion. As a consequence, the color characteristics can offer an easy visual detection method in the colorimetric screening, compared with the monochromatic color change seen in typical colorimetric assays. Furthermore, in a preliminary experiment, there was little variation between observers ($n=6$) in distinguishing between the purple color and the other colors resulting from the complex formation.

The color change resulted from a mixture of free XO and Fe(III)–XO complexes in forms of ML and M_2L, where L and M denote XO and Fe(III) ion, respectively. Free XO, ML complex, and M_2L complex have absorption maxima around 430, 555, and 585 nm, respectively, which produce yellow, red, and purple colors, respectively. The color change from yellow to purple was visually observed when the Fe(III) concentration exceeded approximately 20 μM for 20 μM XO. Figure 1c shows the calculated molar fractions of these species as a function of Fe(III) concentration at a constant XO concentration (20 μM). For this calculation, the formation constants were obtained from a previous report [29]. The M_2L complex formation is due to the sterically isolated two metal-binding sites of XO (Fig. 1a). Each binding site is composed of iminodiacetate and hydroxy (or carbonyl) groups. The binding of the hydroxy group to Fe(III) is also likely responsible for the development of the purple color. At Fe(III) concentrations below 20 μM, the major species are L and ML. The M_2L complex is predominant above approximately 25 μM. Consequently, the purple color is due to the M_2L complex formation and the yellowish or reddish color is mainly due to the ML complex formation in the presence of free XO (Fig. 1b, c). Then, the color change is attributed to the M_2L complex rather than the ML complex. The formation of the

M_2L complex should therefore be the key feature of this assay method.

The M_2L complex formation was examined by varying the H_2O_2 concentration in the presence of 20 μM XO and 40 μM Fe(II). It is noted that the Fe(II) concentration needed to be twice or more that of the XO concentration to obtain a purple color, as described above. The formation of the complex having an absorption maximum at 585 nm was observed with increasing H_2O_2 concentration. The molar absorption coefficient (25,000 M^{-1} cm^{-1} at 585 nm) of the M_2L complex formed under these conditions was less than the coefficient (37,500 M^{-1} cm^{-1}) resulting from simply Fe(III) and XO. The complex formed was monitored by measuring the absorbance at 585 nm. As shown in Fig. 2, the absorbance increased with H_2O_2 concentration up to 20 μM and then reached a maximum value, although the absorbance then decreased slightly. In the visual observation, the reaction mixture had a purple color at H_2O_2 concentrations above 16 μM, while the mixture had a yellow or reddish-yellow color below this concentration. The bending point shown in Fig. 2 suggests the stoichiometry of Fe(II) oxidation by H_2O_2: the bending point around 18 μM H_2O_2 indicates that 1 mol H_2O_2 likely generates approximately 1.7 mol Fe(III) because the bending point appeared around 30 μM Fe(III) in the Fe(III)–XO system. The stoichiometry was almost consistent with that of a previous report [28].

As described above, the H_2O_2 concentration of 16 μM represents the lowest concentration at which the purple color was observed for the XO concentration of 20 μM. This lowest H_2O_2 concentration can be regarded as the boundary concentration to observe the color change from yellow to purple for a given XO concentration. The boundary concentration would differ with XO concentration. Furthermore, when the XO concentration is fixed, not only the H_2O_2 concentration required for the color change but also the pyruvate concentration to be accumulated will be defined. The boundary concentrations were examined
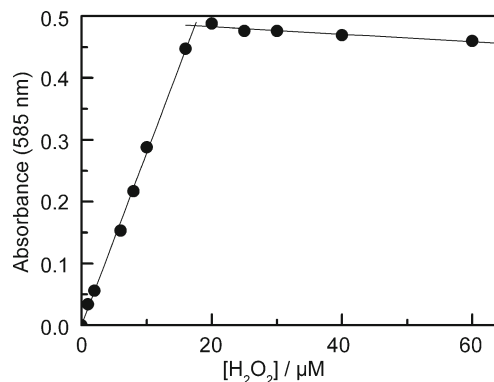
Fig. 2 M_2L complex formation at various concentrations of H_2O_2 in the presence of 40 μM Fe(II) and 20 μM XO

for various XO concentrations. For the current study, the boundary concentration was visually and photometrically defined: the boundary concentration is the lowest H_2O_2 concentration at which the purple color was visually detected and at which the maximum absorbance value was obtained, when increasing the H_2O_2 concentration at a given XO concentration. Also, an Fe(II) concentration twice as high as the XO concentration was used for each XO concentration. Figure 3 shows the boundary concentration plotted as a function of XO concentration. The boundary concentration increased with increasing XO concentration below 100 μM. At higher XO concentrations, further study was not carried out because of the great absorbance value in excess of 1.5. This indicates that H_2O_2 below 100 μM can be detected with the Fe(III)–XO system. In the visual observation of the solutions prepared for the current study, the distinct color was observed at XO concentrations above 20 μM. In addition, XO concentrations above 60 μM provided deep and dark colors, which leads to difficulties to discriminate the resulting color; therefore, the XO concentration of 20 μM was chosen for this assay.

When the indicator reaction is coupled to the enzymatic amplification reaction, Fe(II) and Fe(III) ions may be masked by enzymes and their substrates. The formation of the M_2L complex was monitored at 585 nm in the presence of those substances. The presence of ATP, AMP, PEP, AK, and PK decreased the absorbance to 88% and the presence of only ATP and AMP decreased the absorbance to 75%. These results indicate that the complex formation was interfered with by ATP and AMP because the presence of the enzymes, of which substrates are ATP and AMP, reduced the interference. The interferences are due to phosphate groups of ATP and AMP. The complex formation was also studied in the presence of phosphate ions. The
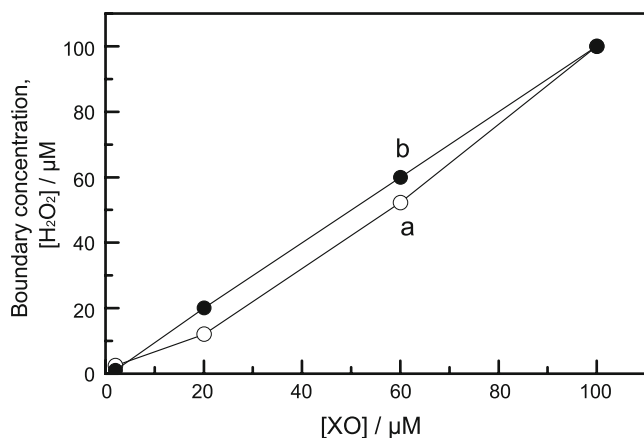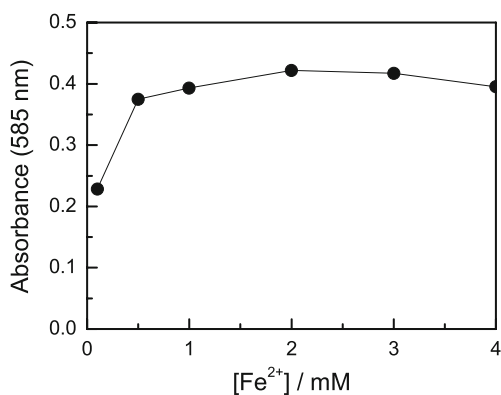
formation of the complex in the presence of 37 mM phosphate was significantly slower than in its absence. Furthermore, the complex formation was not observed at phosphate concentrations above 200 mM. Thus, a phosphate buffer is unsuitable for use in the amplification reaction (pH 7.8). Besides the interference of phosphate, the oxidation of Fe(II) ion by H_2O_2 is inherently slow. The interferences of ATP and AMP and the slow oxidation could be improved by using higher concentrations of Fe(II) ion. The effect of Fe(II) ion concentration on the color development was studied in the presence of ATP, AMP, AK, and PK. For this study, after pyruvate oxidase reaction with 12.5 μM pyruvate, the H_2O_2 generated was reacted with various concentrations of Fe(II) ion, in the presence of 20 μM XO at pH 2.0 and the mixtures were incubated for 15 min. Then, the absorbance of the complex formed was measured at 585 nm. Figure 4 shows absorbance plotted as a function of Fe(II) concentration. The absorbance increased with increasing Fe(II) concentration and reached a maximum value around 2 mM. At 2 mM Fe(II), the time course of the complex formation was measured, and showed a plateau at 5 min. Then, an Fe(II) concentration of 2 mM and a reaction time of 5 min were selected for the complex formation. Also, ACES buffer was chosen for the amplification reaction because an ACES buffer exhibited no interferences in the complex formation. Adenine nucleotides and phosphate from most of the samples would not interfere with the complex formation because the Fe(II) concentration employed is much higher than their concentrations. Finally, when a purple color was observed at 20 μM XO and 2 mM Fe(II) in the presence of enzymes and substrates, the absorbance value at 585 nm was more than approximately 0.35. This absorbance value represents the boundary for the color change from yellow to purple.

The time required for the pyruvate oxidase reaction was examined. To obtain the time course of H_2O_2 production in the pyruvate oxidase reaction, the mixture was incubated for different times. After the 2-mL portion of the mixture had reacted with the Fe/XO reagent (2 mL), the absorbance at 585 nm was measured. The absorbance reached a plateau at 5 min and thus the reaction time of 5 min was chosen for the pyruvate oxidase reaction.

The indicator reaction was coupled to the amplification reaction. Figure 5 shows the progress curves of the amplification reaction obtained with initial ATP concentrations of 0, 0.2, 0.5, and 5.0 nM. For these progress curves, after the amplification reaction had been initiated, portions of the reaction mixture were taken at intervals of 15 min. Then, the indicator reaction was carried out and the resulting color was monitored by measuring the absorbance at 585 nm. The absorbance data were fitted to a sigmoid curve using Origin Pro 7.5 because the amplification reaction shows a sigmoid progress curve [14]. As shown

Fig. 3 Boundary concentrations of H_2O_2 for the color change defined visually (**a**) and photometrically (**b**) at various XO concentrations. For each data point, the Fe(II) concentration used was twice as high as that of XO

Fig. 4 Effect of Fe(II) concentration on Fe(III)–XO complex formation in the presence of enzymes and their substrates. To the solution composed of 50 μM adenosine 5′-triphosphate (ATP), 50 μM pyruvate, 100 μM adenosine 5′-monophosphate (AMP), 1.86 U/mL adenylate kinase (AK), 1.86 U/mL pyruvate kinase (PK), and 0.15 M N-(2-acetamido)-2-aminoethanesulfonic acid (ACES) at pH 7.8 (2.0 mL), 0.36 mM HCl (320 μL), and 8.81 U/mL pyruvate oxidase (680 μL) were added. After the incubation for 5 min, the mixture was reacted with Fe(II) and 20 μM XO at pH 2.0 for 15 min

in Fig. 5, the progress curves had the same constant plateau at given AMP and PEP concentrations. The progression of the amplification reaction at 0 nM ATP is possibly due to ATP or ADP contained in the reagents used.

To examine the effect of AMP and PEP concentrations on the kinetics of the amplification reaction, the time to reach half of the plateau of the progress curve for a given concentration of ATP was defined as $T_{1/2}$. The difference in $T_{1/2}$ between two ATP concentrations ($\Delta T_{1/2}$) is associated with the sensitivity and accuracy when the resulting colors for the two concentrations are discriminated visually. A significantly small $\Delta T_{1/2}$ indicates that the progress curves are overlapped
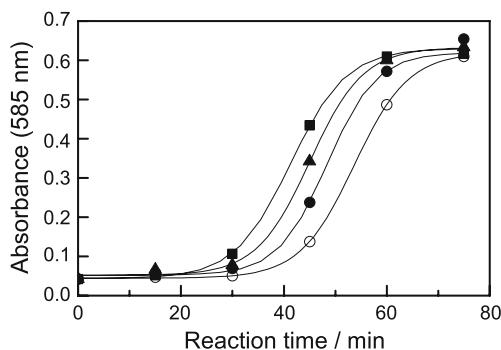
Fig. 5 Progress curves of the amplification reaction. The points represent the experimental data obtained at initial ATP concentrations of 0 mM (*open circles*), 0.2 nM (*filled circles*), 0.5 nM (*triangles*), and 5.0 nM (*squares*). The *lines* represent fitting sigmoid curves produced by with the software program used to produce the plot. Amplification conditions were as follows: 50 μM AMP, 500 μM phosphoenol pyruvate (PEP), 1.9 U/mL AK, 1.9 U/mL PK, 0.15 M ACES; pH 7.8. For the pyruvate oxidase reaction the conditions were as follows: 6.0 U/mL pyruvate oxidase; incubation, 5 min; pH 5.5. For the complex formation the conditions were as follows: 20 μM XO, 2 mM Fe(II); incubation, 5 min; pH 2.0

or very close to each other, which results in difficulties in the discrimination of the resulting color; therefore, a large $\Delta T_{1/2}$ is favorable for the visual detection in this assay. $T_{1/2}$ and $\Delta T_{1/2}$ are related to the reaction rate of the AK/PK cycling reaction and thus depend on AMP and PEP concentrations. $\Delta T_{1/2}$ was examined by varying AMP and PEP concentrations. For this study, $T_{1/2}$ values for 0 and 50 nM ATP were obtained by reading the time on the fitted progress curves for 0 and 50 nM. The progress curves were obtained at various AMP concentrations with 500 μM PEP. $T_{1/2}$ increased with decreasing AMP concentration because of the reduction in the reaction rate. Figure 6a shows the change of $\Delta T_{1/2}$ as a function of AMP concentration at a PEP concentration of 500 μM. $\Delta T_{1/2}$ increased with decreasing AMP concentration. In addition, a large increase of $\Delta T_{1/2}$ was observed in the range 10–100 μM.

The absorbance value at the plateau of the progress curves was also dependent on AMP and PEP concentra-
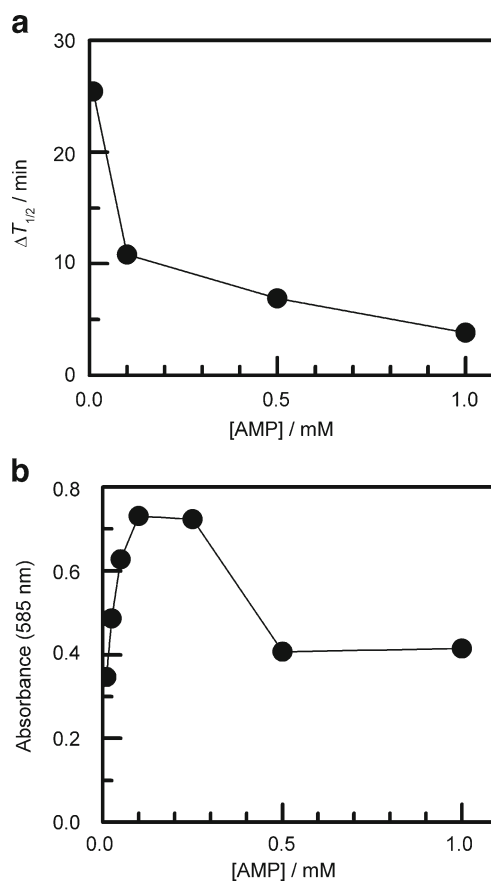
Fig. 6 a $\Delta T_{1/2}$ versus AMP concentration and **b** effect of AMP concentration on complex formation. The ATP concentrations were as follows: 0 and 50 nM (**a**) and 0.5 nM (**b**). The amplification conditions were as follows: 500 μM PEP, 1.9 U/mL AK, 1.9 U/mL PK, 0.15 M ACES; pH 7.8. For the pyruvate oxidase reaction the conditions were as follows: 6.0 U/mL pyruvate oxidase; incubation, 5 min; pH 5.8. For the complex formation the conditions were as follows: 20 μM XO, 2 mM Fe(II); incubation, 5 min; pH 2.0

tions. This value has to be greater than 0.35 because the color change occurs at an absorbance value above 0.35 for 20 μM XO used in the indicator reaction. The plateau value (absorbance at 585 nm) was examined with various concentrations of AMP and 500 μM PEP. The absorbance increased with increasing AMP concentration up to 250 μM and then decreased (Fig. 6b). The absorbance also exceeded 0.35 at AMP concentrations above 25 μM. The decease in absorbance is possibly due to the production of excess H_2O_2 that leads to decomposition of XO and Fe (III)–XO complexes. With 50 μM AMP, the absorbance was measured at various concentrations of PEP. The absorbance exhibited a constant value in the range 200–1,000 μM. Consequently, 50 μM AMP and 500 μM PEP were used for the amplification reaction.

In this method, the reaction time of the pyruvate amplification can be fixed so that a purple color is observed above a given criterion (ATP concentration). Typically, the intersection point between the progress curve for a concentration criterion and the absorbance of 0.35 corresponds to the time for the amplification reaction. Here, it is noted that each fixed criterion is detected with the same sensitivity for an absorbance of 0.35. For screening criteria of 0.5 and 5.0 nM ATP, the amplification reaction times were 45 and 40 min, respectively. The lowest criterion (the LOD of this assay) that could be fixed in this assay method was 0.5 nM. At lower concentrations, the blank reaction without ATP exhibited a purplish color and then color discrimination by visual observation was difficult above and below a criterion. However, the LOD of 0.5 nM was lower than those of the colorimetric assay and molecular sensors previously reported [7–11]. Since a trace amount of contaminants such as ATP and ADP is responsible for the blank reaction, the LOD will be decreased if they are further reduced in the preparation of the assay solutions. Finally, the total assay time was approximately 60 min. The assay time was long compared with the time for the bioluminescence assay although the cultivation-based test kits need a much longer time. The long assay time can be compensated for by performing a parallel assay with a 96-well microtiter plate, which would result in significant improvement of the assay throughput.
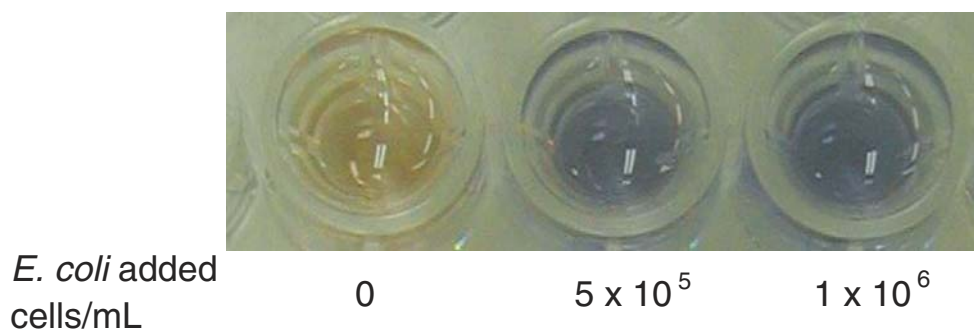
The reproducibility for 0 and 5.0 nM ATP was examined by measuring the absorbance at 585 nm after the amplification reaction for 40 min and the indicator reaction. The relative standard deviations were 15 and 13% for 0 and 5.0 nM, respectively ($n=5$). In visual observation there was no noticeable difference in the resulting color for each run at the same concentration. The precision of the present assay would be sufficient for screening purposes although the assay system needs to be improved for a precise assay. The colors formed were stable for at least 60 min after the assay. The stability of the color formed is likely satisfactory for performing a visual detection task even though a large number of assays are performed in parallel.

Assay of ATP extracted from *E. coli*

The utility of this method was tested with food samples containing *E. coli*. The samples were prepared by adding known concentrations of *E. coli* cells to commercially available cow milk to give 0, 5×10^5, and 1×10^6 cells/mL in the amplification reaction. These *E. coli* concentrations correspond to 0, 0.5, and 1.0 nM ATP, respectively, in the amplification reaction. The samples were treated with 5% trichloroacetic acid and the mixtures were centrifuged. Then, the neutralized supernatant was assayed using the current method with a concentration criterion of 0.5 nM ATP. The amplification reaction required a longer time because trichloroacetic acid is a potent inhibitor of enzymes. However, as shown in Fig. 7, the difference in color was clearly observed in the real samples and a purple color was observed with samples at cell numbers above 5×10^5 cells/mL. This indicates that the assay of ATP extracted from *E. coli* in one of the food samples was successfully performed using this method. The use of mechanical cell disruption, such as sonication and homogenization, would allow the assay without inhibition of enzyme activities.

Conclusions

In the study reported here, a colorimetric method for the screening assay of ATP was developed. The use of an

Fig. 7 Assay of ATP extracted from *Escherichia coli* cells that had been added to commercially available cow milk

E. coli added cells/mL

0   5×10^5 1×10^6

enzymatic amplification reaction and Fe(III)–XO complex formation offered a clearly distinct color change, i.e., yellow to purple, for a nanomolar level of ATP. This assay method was successfully applied to the assay of ATP extracted from *E. coli* added to cow milk. Besides the visual colorimetry, this assay would also allow one to quantitatively monitor the cell number in food manufacturing by measuring the absorbance at 585 nm with a simple colorimetric apparatus routinely used in the workplace.

References

1. Niza-Ribeiro J, Louzã AC, Santos P, Lima M (2000) Food Control 11:209–216
2. Davidson CA, Griffith CJ, Peters AC, Fielding LM (1999) Luminescence 14:33–38
3. Champiat D, Matas N, Monfort B, Faass H (2001) Luminescence 16:193–198
4. Siragusa GR, Cutter CN, Dorsa WJ (1995) J Food Prot 58:770–775
5. Reybroeck W (1997) In: Stanley PE, Smither R, Simpson WJ (eds) A practical guide to industrial uses of ATP-luminescence in rapid microbiology. Cara Technology, Lingfield
6. Ishida A, Yoshikawa T, Nakazawa T, Kamidate T (2002) Anal Biochem 305:236–241
7. Worthy E, Whitehead P, Goldberg DM (1970) Enzymol Biol Clin 11:193–210
8. Horgan DJ (1978) Aust J Biol Sci 31:21–24
9. Sancenón F, Descalzo AB, Martínez-Máñz R, Miranda MA, Soto J (2001) Angew Chem Int Ed 40:2640–2643
10. Li C, Numata M, Takeuchi M, Shinkai S (2005) Angew Chem Int Ed 44:6371–6374
11. Jose DA, Mishra S, Ghosh A, Shrivastav A, Mishra SK, Das A (2007) Org Lett 9:1979–1982
12. Breckenridge BM (1964) Proc Natl Acad Sci USA 52:1580–1586
13. Valero E, Varón R, García-Carmona F (2004) Biophys J 86:3598–3606
14. Chittock RS, Wharton CW, Jackson JB, Berovic N, Benyon D (1991) Biochem Soc Trans 19:160S
15. Hawronskyj JM, Chittock RS, Holah J, Wharton CW (1994) In: Campbell AK, Kricka LJ, Stanley PE (eds) Bioluminescence and chemiluminescence—fundamentals and applied aspects. Wiley, Chichester, pp 411–414
16. Campell J, Chang TMS (1975) Biochim Biophys Acta 397:101–109
17. Chittock RS, Hawronskyj JM, Holah J, Wharton CW (1998) Anal Biochem 255:120–126
18. Valero E, Varón R, García-Carmona F (2000) Biochem J 350:237–243
19. Wimmer MC, Artiss JD, Zak B (1986) Clin Chem 32:629–632
20. Fossati P, Prencipe L, Berti G (1980) Clin Chem 26:227–231
21. Tamaoku K, Murao Y, Akiura K (1982) Anal Chim Acta 136:121–127
22. Ishida A, Kaneko E, Yotsuyanagi T (1999) Chem Lett 28:351–352
23. Gupta BL (1973) Microchem J 18:363–374
24. Jiang ZY, Woolard AC, Wolff SP (1990) FEBS Lett 268:69–71
25. Jiang ZY, Woollard AC, Wolff SP (1991) Lipids 26:853–856
26. Jiang ZY, Hunt JV, Wolff SP (1992) Anal Biochem 202:384–389
27. Wolff SP (1994) Methods Enzymol 233:182–189
28. Gay C, Collins J, Gebicki JM (1999) Anal Biochem 273:149–155
29. Mizuguchi H, Atsumi H, Hashimoto K, Shimada Y, Kudo Y, Endo M, Yokota F, Shida J, Yotsuyanagi T (2004) Anal Chim Acta 527:131–138